Aptamer-based assay for monitoring genetic disorder phenylketonuria (PKU)

Mohammad Hasanzadeh, Amir Zargami, Hossein Navay Baghban, Ahad Mokhtarzadeh, Nasrin Shadjou, Soltanali Mahboob

PII: S0141-8130(18)31591-5
DOI: doi:10.1016/j.ijbiomac.2018.05.028
Reference: BIOMAC 9629

To appear in:

Received date: 5 April 2018
Revised date: 5 May 2018
Accepted date: 5 May 2018

Please cite this article as: Mohammad Hasanzadeh, Amir Zargami, Hossein Navay Baghban, Ahad Mokhtarzadeh, Nasrin Shadjou, Soltanali Mahboob , Aptamer-based assay for monitoring genetic disorder phenylketonuria (PKU). The address for the corresponding author was captured as affiliation for all authors. Please check if appropriate. Biomac(2017), doi:10.1016/j.ijbiomac.2018.05.028

Aptamer-based assay for monitoring genetic disorder phenylketonuria (PKU)

Mohammad Hasanzadeh [a*], Amir Zargami [b], Hossein Navay Baghban [c], Ahad Mokhtarzadeh [d], Nasrin Shadjou [e], Soltanali Mahboob [b]

d

[a] Drug Applied Research Center, Tabriz University of Medical Sciences, Tabriz, Iran.

[b] Department of Biochemistry, Higher Education Institute of Rab-Rashid, Tabriz, Iran.

[c] Pharmaceutical Analysis Research Center, Tabriz University of Medical Sciences, Tabriz, Iran.

[d] Immunology Research Center, Tabriz University of Medical Sciences, Tabriz, Iran.

[e] Department of Nanochemistry, Nano Technology Research Center, Uremia University, Uremia 57154, Iran.

Corresponding Author

E-mail address: (*) hasanzadehm@tbzmed.ac.ir

Drug Applied Research Center, Tabriz University of Medical Sciences, Tabriz 51664, Iran.

Tel: +98(41) 33363311; Fax: +98(41)33363231

Abstract

The genetic disorder phenylketonuria (PKU) is the inability to metabolize phenylalanine because of a lack of the enzyme phenylalanine hydroxylase. Phenylalanine is used to biochemically form proteins, coded for by DNA. The development of an apta-assay for detection of L-Phenylalanine is presented in this work. A highly specific DNA-aptamer, selected to L-Phenylalanine was immobilized onto a gold nanostructure and electrochemical measurements were performed in a solution containing the phosphate buffer solution with physiological pH. We have constructed an aptamer immobilized gold nanostructure mediated, ultrasensitive electrochemical biosensor (Apt/AuNSs/Au electrode) for L-Phenylalanine detection without any additional signal amplification strategy. The aptamer assemble onto the AuNSs makes Apt/AuNSs/Au electrode an excellent platform for the L-Phenylalanine detection in physiological like condition. Differential pulse voltammetry were used for the quantitative L-Phenylalanine detection. The Apt/AuNSs/Au electrode offers an ultrasensitive and selective detection of L-Phenylalanine down to 0.23 µM level with a wide dynamic range from 0.72 µM-6 mM. The aptasensor exhibited excellent selectivity and stability. The real sample analysis was performed by spiking the unprocessed human serum samples with various concentration of L-Phenylalanine and obtained recovery within 2% error value. The sensor is found to be more sensitive than most of the literature reports. The simple and easy way of construction of this apta-assay provides an efficient and promising diagnosis of phenylketonuria.

Keyword; aptamer; genetic disorder; biomarker; phenylketonuria; gold nanostructure

1. Introduction

The genetic disorder phenylketonuria (PKU) is the inability to metabolize phenylalanine (Phe) because of a lack of the enzyme phenylalanine hydroxylase. Phenylketonuria (PKU) is an inborn error of metabolism that results in decreased metabolism of the amino acid phenylalanine. Untreated PKU can lead to intellectual disability, seizures, behavioral problems, and mental disorders. It may also result in a musty smell and lighter skin. Babies born to mothers who have poorly treated PKU may have heart problems, a small head, and low birth weight.[1]

Phenylalanine is used to biochemically form proteins, coded for by DNA. L-Phe is classified as neutral, and nonpolar because of the inert and hydrophobic nature of the benzyl side chain. The L-isomer is used to biochemically form proteins, coded for by DNA. The codons for L-Phenylalanine are UUU and UUC. Phenylalanine is a precursor for tyrosine; the monoamine neurotransmitters dopamine, norepinephrine (noradrenaline), and epinephrine (adrenaline); and the skin pigment melanin [2].

Some analytical methods such as capillary electrophoresis, chromatography, mass spectrometry, ion exchange column chromatography, spectrophotometry and fluorometry are the most widely used methods for detection of Phe [3-7]. These techniques may not be well-suited for routine clinical screening of Phe, as they are often time consuming and require some tedious preparation and expensive equipment.

Since the pioneering studies on aptamers [8], substantial research efforts have been directed in order to apply the aptamers as the bioreceptor in different detection schemes such as micro gravimetric [9], and electrochemical aptasensors [10-12]. Aptamers are artificial nucleic acid ligands showing specific binding affinity for amino acids, drugs, proteins and other molecules, which can be screened through the systematic evolution of ligands by exponential

enrichment (SELEX) process from random RNA or DNA libraries [8]. Compared with antibodies, aptamers possess some outstanding features, including high specificity of binding affinity, nice stabilization, easy synthesis and modification with electrochemical active markers, optical dyes, enzymes and other desired substances. Furthermore, aptamers can reversibly capture and release their target molecule. It is more facile for the aptamer to transduce the recognition events in to detectable signals [13].

The fabrication of aptamer-based electrochemical biosensors as an emerging technology has made the detection of small and macromolecular analytes easier, faster, and more suited for the ongoing transition from fundamental analytical science to the early detection of protein biomarkers. In the fabrication of aptamer-based electrochemical biosensors, one of the most popularly used electrode materials is gold, upon which thiolated DNA/RNA strands can be immobilized via strong Au-S linkages [14, 15]. The modification of DNA or RNA with a terminal thiol is straightforward: simple phosphoramidite chemistry on the DNA/RNA synthesizer suffices. The modification of Au surfaces with the thiolated oligonucleotide strands is readily accomplished by dipping a cleaned Au slide into the deposition solution to form an aptamer layer. Although the initial adsorption of thiolated DNA strands onto gold surfaces occurs within minutes, it is necessary to allow the reaction to continue for up to 24 h to ensure a homogenous surface. The resulting surface is usually subjected to a passivation step (*i.e.,* treated with 1-mercapto-6-hexanol solution) to minimize non-specifically bound oligonucleotide strands [16-19].

In the present study, at continuation of our studies on detection of lower concentration of amino acids using electrochemical sensors [9-11 and 20-24] we investigated a biosensor based on aptamer immobilized on the surface of AuNSs modified gold electrode for simple, sensitive, rapid and cost-effective determination of L-phenylalanine (Phe). To the best our knowledge, this device is the first aptasensor based on AuNSs for selective detection of L-

Phe which has not been previously reported. This report is the first example of L-Phe aptamer-based electrochemical sensor using AuNSs.

2. Experimental

2.1. Reagent and chemicals

5' Thiolated L-Phe aptamer modification was custom-synthesized by Takapu Zist Co. (Iran) and its base sequence is as follows: 5'-SH-GCGCGAGAAACGGUCACUAGAAUAGUGGGCCGUCAUGCUAACGCCUCUUUCGGUGUUGGGGGAAUAUUGGCCAAUCGAGU-3'.

2-Mercaptoethanol was purchased from Sigma Aldrich (USA). All solutions were prepared with bidistilled water. Potassium ferrocyanide $K_4Fe(CN)_6$, potassium ferricyanide $K_3Fe(CN)_6$, hydrochloric acid, bovine serum albumin (BSA), sulfuric acid, 1-ethyl-3-(3-dimethylaminopropyl) carbodiimide hydrochloride(EDC), N-hydroxysuccinimide (NHS), cysteamine hydrochloride, hydrogen tetrachloroaurate(III)hydrate ($HAuCl_4 \cdot 3H_2O$), were obtained from Sigma-Aldrich (Ontario, Canada). Other chemicals used in this work were of analytical reagent grade, from Merck (Germany). CTAB, cetyltrimethylammonium bromide (Ranchem) dissolved in water plays a dual role as a supporting electrolyte and a surfactant to stabilize AuGQs). All the solutions were prepared using Millipore water (18.2MΩ.cm) and the temperature maintained throughout the study is 25 ^{o}C.

2.2.Apparatus

Electrochemical measurements were carried out in a conventional three-electrode cell (from Metrohm) powered by an electrochemical system comprising of AUTOLAB system with PGSTAT 302N (Eco Chemie, Utrecht, The Netherlands). The system was run on a PC using NOVA 1.11 software. The ac voltage amplitude used was 10 mV and the equilibrium time was 5 s. An Ag/AgCl-Sat'd KCl (from Metrohm) and a platinum wire were used as reference

and counter electrodes, respectively. The working electrode was a gold (Au) electrode (d=2mm) (from Azar Electrode Co., Urumia, Iran). For differential-pulse voltammetry (DPV) measurements, a pulse width of 25 mV, a pulse time of 50 ms, and a scan rate of 100 mV s^{-1} were employed. All the electroanalytical tests were carried out at 25 °C in 10 mM Tric-HCl buffer (pH=7.4). The surface morphology of electrode surface was characterized by high-resolution field emission scanning electron microscope (FE-SEM, Hitachi-SU8020, Czech) with an operating voltage of 3 kV, and chemical compositions of the AuNSs were analysed by an energy dispersive spectroscopy (EDS) coupled with the FE-SEM equipment. TEM (transmission electron microscopy) analysis was conducted on a Philips CM30 electron microscope operated at 200 kV (Adelaide, Australia). Atomic force microscopic (AFM) analysis was carried out by Nanosurf (AG Gräubernstrasse 124410 Liestal Switzerland) in a tapping mode to confirm the surface immobilization of aptamers on the substrates.

2.3.Preparation of aptasensor

Before modification, gold disk electrode was polished with alumina slurry (0.3 µm and 0.05 µm) and washed thoroughly with water. The freshly polished electrode was then sonicated in ethanol followed by DI water for a couple of times. Further, cleaning was carried out by potential cycling between -0.3 V and 0.8 V in 0.1 M H_2SO_4 at a scan rate of 100 mV/s for 20 cycles. This is followed by sonication of electrode for 2 min in DI water and dried before modification. AuNSs modified gold electrode was prepared by cycling in the potential range from 0 V to 1.2 V for 20 times in aqueous CTAB solution (50 mM) at a scan rate of 100 mV/s. The cyclic voltammogram of the deposition is given in Fig. S1.

2.4. Electrogeneration of Au NSs

The potential cycling of the polycrystalline gold disk electrode in either 50 mM or 0.1mM CTAB solution for 50 consecutive runs) in a potential region from 0 to 1.2 V *vs.* Ag/AgCl for 50 cycles at a scan rate of 100 mVs^{-1} leads to the formation Au NSs film on the

surface of the gold disk electrode. Then the electrode is washed using water and dried. The electrode coated with Au NSs film is then utilized for the electrocatalytic reaction. In the same way the Au NSs is coated on the Au electrode for voltammetric studies.

The Au NSs modified Au electrode was rinsed with water and dried in air. The concentration and incubation time for aptamer to obtain the complete coverage of the Au NSs/Au surface was optimized. 2 µM concentration of aptamer with an incubation time of 1h is found to be adequate to produce a complete surface coverage on Au NSs/Au electrode. 10 µL of 2 µM aptamer was immobilized on Au NSs/Au electrode by drop casting and kept for drying at 25 °C for 1 h. The electrode was again washed with DI water to remove the unbounded aptamer and the Apt/Au NSs/Au electrode dried in air. Further, the final electrode (Apt/Au NSs/Au) was immersed in 0.1 mM MCH for 16min, in order to avoid the nonspecific binding of analyte, and again rinsed with DI water and dried in air. The Apt/Au NSs/Au electrode was used for the detection of L-Phe. A schematic diagram depicting the fabrication and working of Apt/Au NSs/Au electrode is shown in Scheme 1.

Low-dimensional materials can be deposited on electrode surfaces using micellar electrodeposition that can be described by a model similar to the one presented by Naoi et al [25]. Based on this model, we suggest a possible mechanism of formation of gold nanostructure that involves the following steps: (**a**) adsorption of micellar Au-CTAB complex on the electrode surface; (**b**) formation on the electrode surface of "hemi-micelles" containing gold nanostructure formed upon electrochemical reduction during the cathodic scan; (**c**) gold nuclei (gold nanostructure, in the present case) surrounded by the stabilizing CTA^+ (during which growth beyond gold nanostructure is stopped by CTAB micelles; (**d**) deposition of more mass of clusters occurs as CTAB monolayers around gold nanostructure are known to be highly disordered [26]; deposition occurs through these defects. Development of layers of surfactant protected clusters occurs,

although limited to a particular thickness, for example, 50 potential cycles in the electrochemical treatment described above. This additional mass of clusters produced is "loosely" held to the electrode surface and can also be collected by repeated scraping off the product from the electrode. As can be explained by this model, the individual clusters are "connected" to the substrate through the defects in the CTAB monolayers. The observation of distribution in the size of the NSs suggests that the control over the size of the NSs is not yet perfect. The deposited layers can also be collected by repeated scraping off the product from the electrode for physical characterization.

We find, during the electrochemical cycling in region from 0.0 to 1.2 V *vs.* Ag/AgCl for 50 cycles at a scan rate of 100 mV/s, during which the AuNSs are produced, that at the end of the 15^{th} cycle itself, the deposit almost stops growing. This could be gauged by the saturation of current growth. However, in order to ensure uniform and maximum level of growth, we chose to employ 50 cycles for deposition. Under these conditions, surely a very adherent film of gold nanostructure is deposited over which additional growth occurs which is loosely bound to the electrode.

10 µM primary aptamer was diluted in 0.1M Tris-HCl buffer (140 mM NaCl, 1 mM $MgCl_2$, pH 7.4). The Au electrode was incubated with primary aptamer at room temperature. Then the blocking reagent MCH was added to the surface of the gold electrode to reduce non-specific adsorption for 1h.

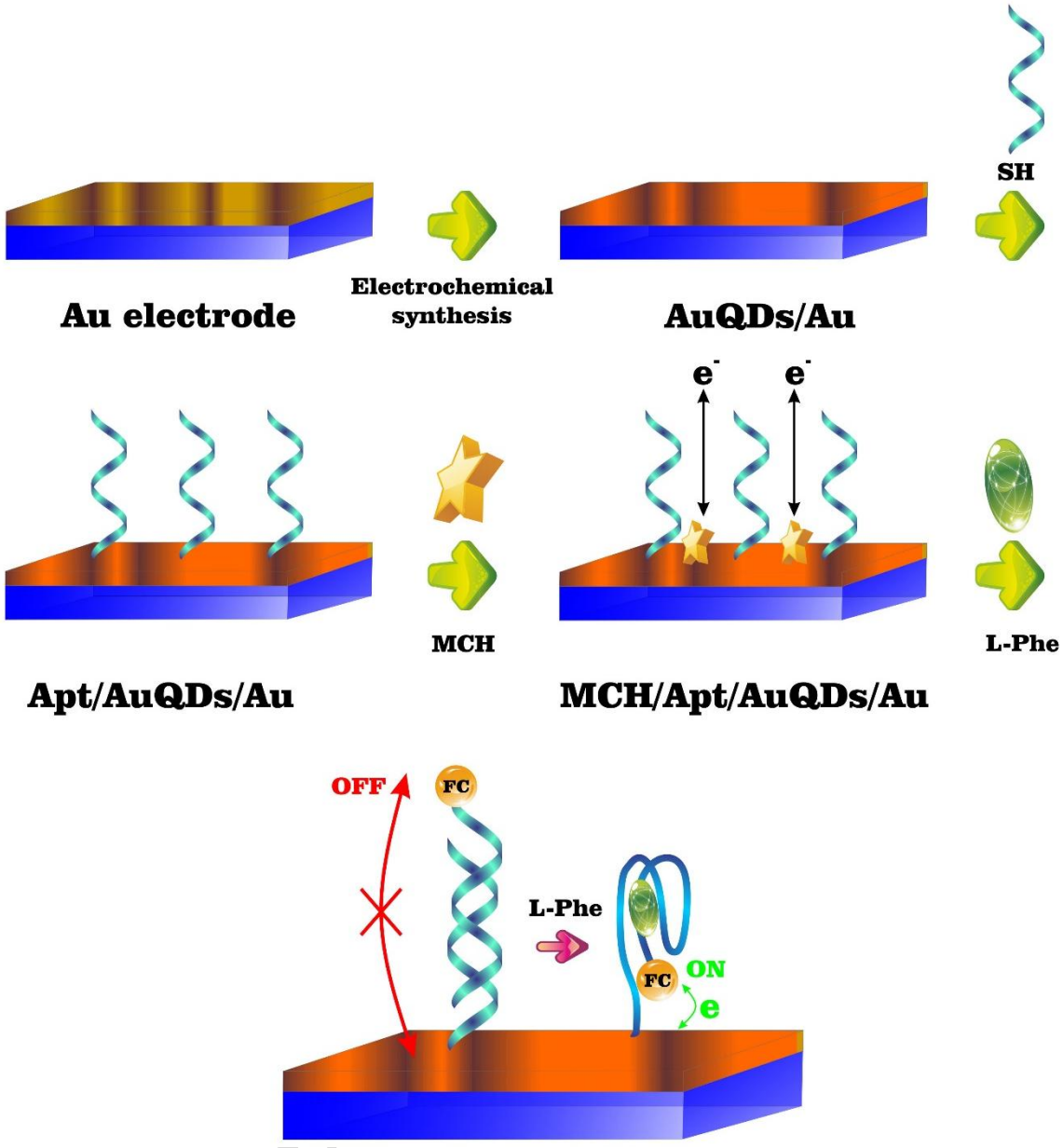

Scheme 1. Schematic representation of the fabrication and working principle of Apt/AuNSs/Au electrode.

2.5. Morphological studies of Au NSs

The electrochemically synthesized Au NSs was characterized by HR-TEM, and EDS. Fig. S2 exhibits the TEM image of Au NSs/Au electrode, which shows the Au NSs with particle size ranging from 1 nm to 5 nm. The structural instability of Au NSs can be attributed to their tendency to aggregate when they are exposed to intense electron beam [27]. Moreover, the

poor contrast exhibited by the TEM images can be account to the presence of sub-nanometer sized entities.

Fig. 3 shows the 2D and 3D AFM height and cross-sectional images for Au electrode after modification with the Au NSs. It's observed that, a non-uniform morphology was appeared after modification of Au electrode by Au NSs. The observed change in non-uniform morphology for Au NSs/Au electrode to uniformly distributed structure for aptamer modified Au NSs/Au confirms the successful formation by thiolated aptamer. These changes could be attributed to aptamer binding making the surface smoother. Fig. 4 shows 2&3D AFM height images before and after aptamer binding to the Au NSs/Au electrode. In contrast to fig. 3, Apt/Au NSs/Au electrode shows one small peak confirming the successful immobilization of phenylalanine specific aptamer on the Au NSs/Au electrode (Fig. 4). Aptamers appeared to be bound uniformly throughout the surface of the Au NSs/Au electrode. Based on the obtained results by AFM, the surface immobilization of aptamers on Au NSs/Au electrode was also shows that of aptamers bound to Au NSs/Au electrode being immobilized at a certain interval. Phenylalanine specific aptamer was thought to be bound all around the AuNSs with a cylindrical morphology, which resulted in different heights in the 3D AFM image (Fig. 4).

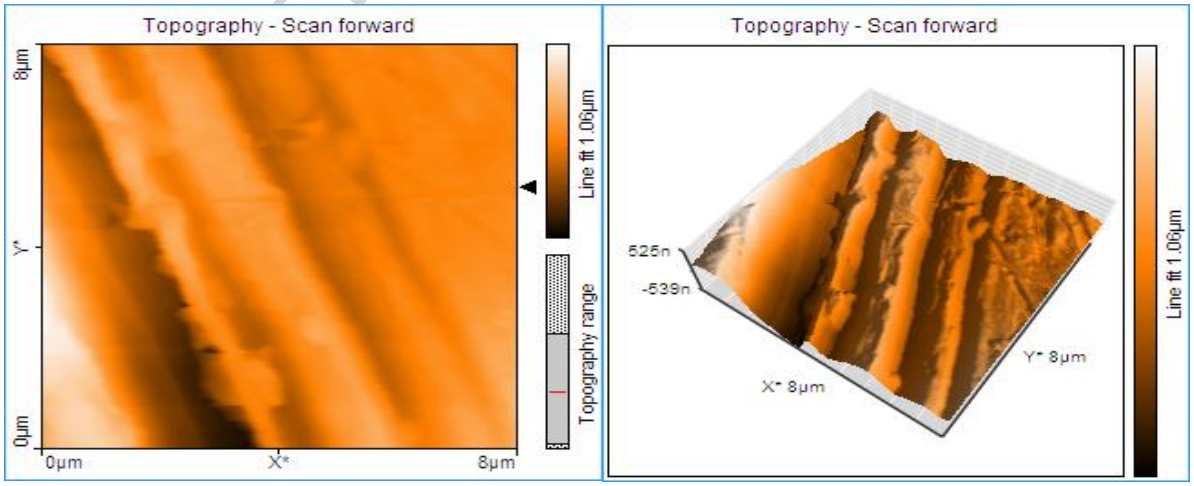

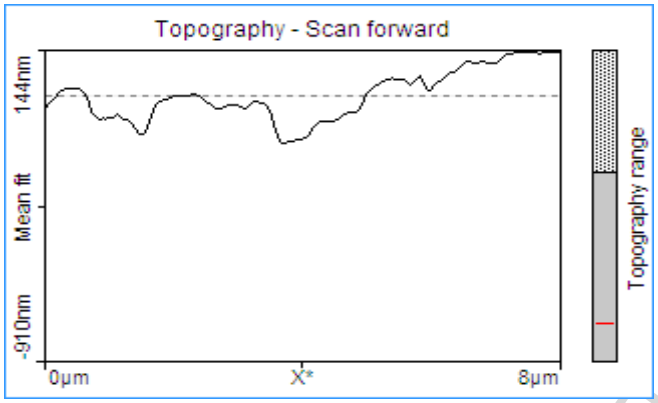

Fig. 3. 2D and 3D AFM height and cross-sectional images for Au electrode after modification with the AuNSs.

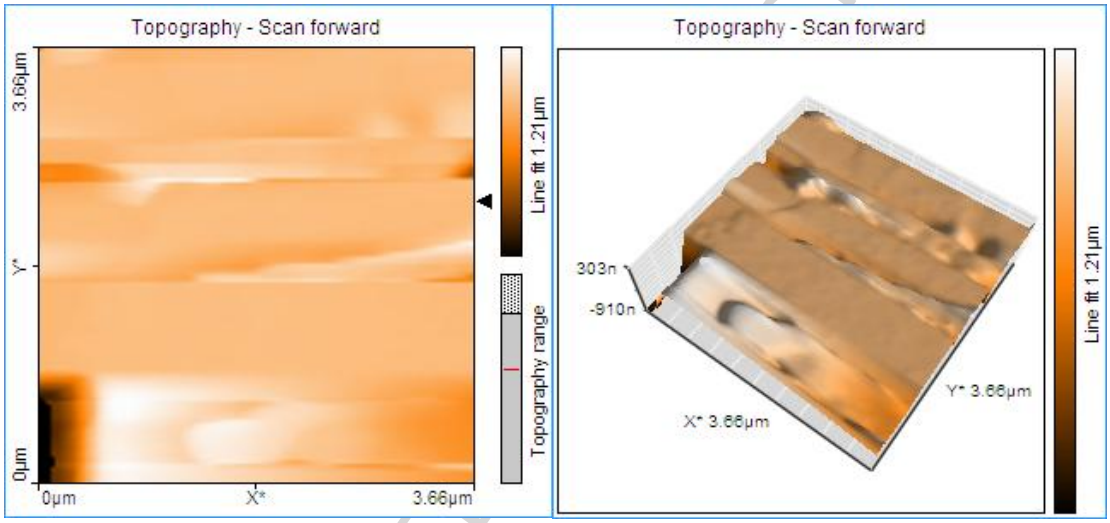

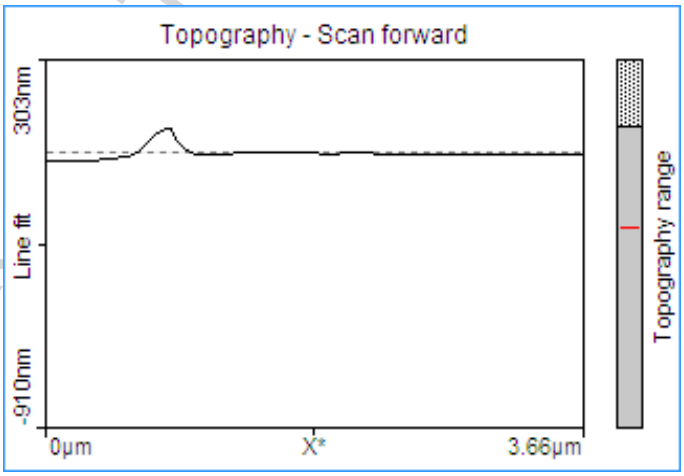

Fig. 4. 2D and 3D AFM height and cross-sectional images for Au/AuNSs after immobilization of phenylalanine specific aptamer.

All of these results were confirmed by SEM and EDS analysis of Au/Au NSs and Apt/AuNSs/Au electrode (Fig. 5).

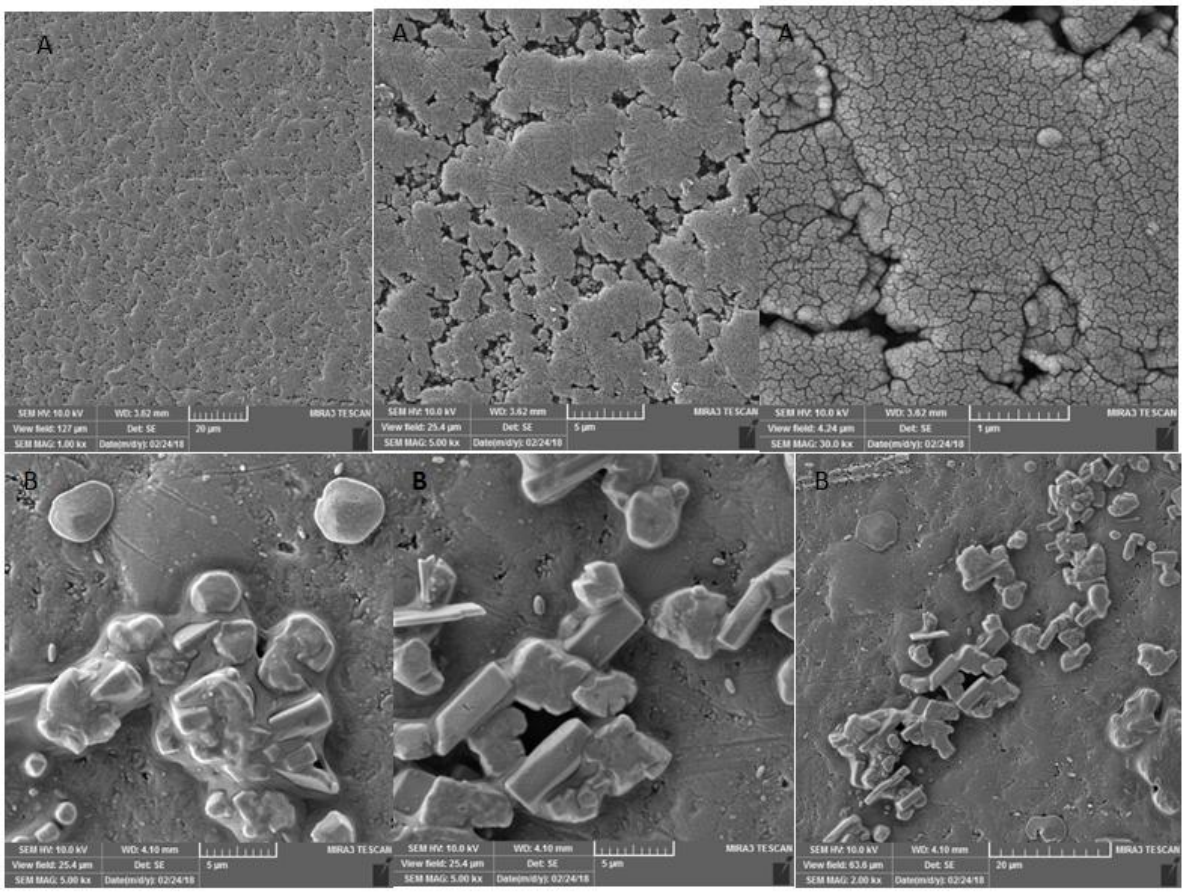

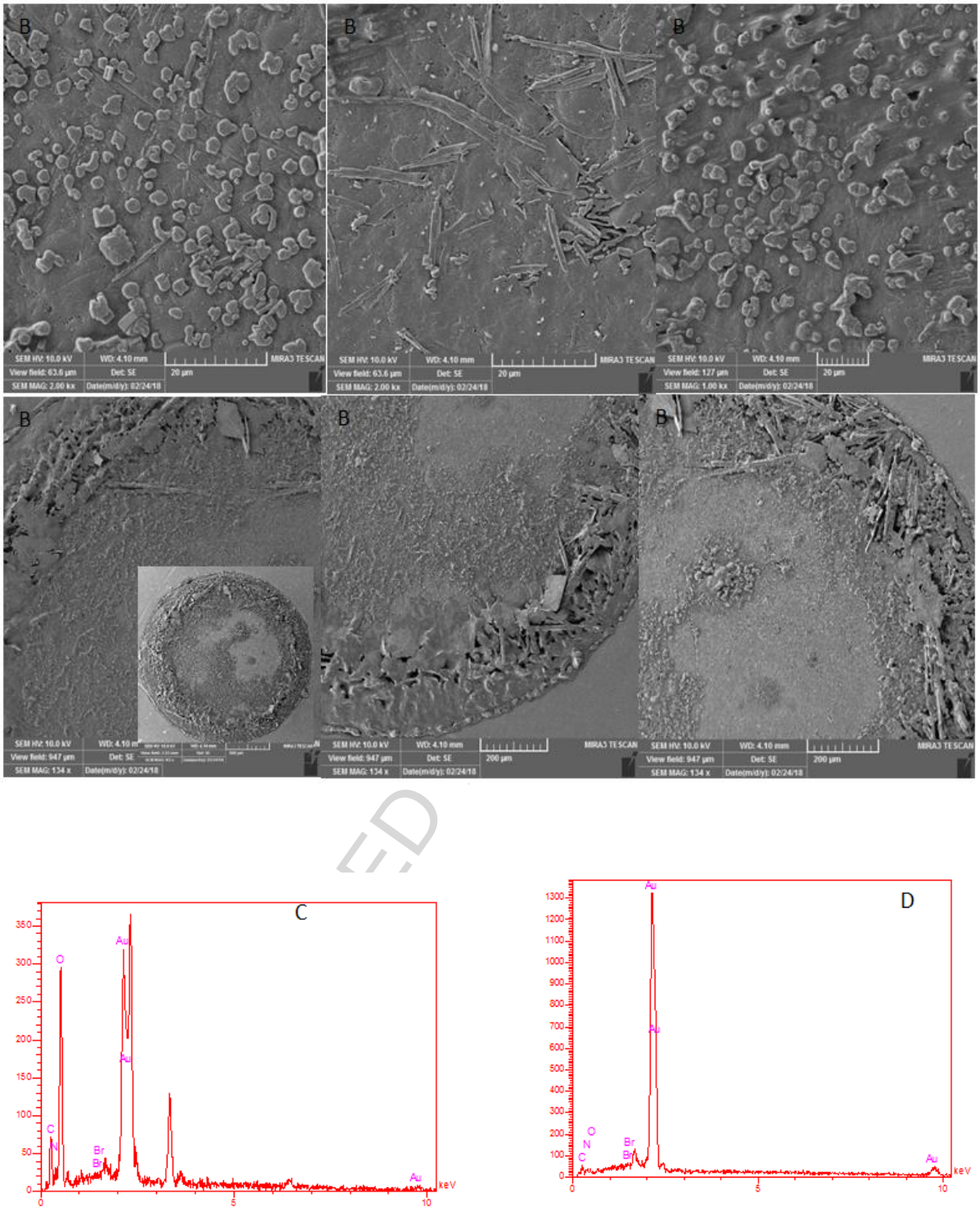

Fig. 5. FE-SEM (**A&B**) and EDS (**C&D**) images of Au/Au NSs and Apt/Au NSs/Au electrode.

3. Results and discussion

3.1. Electrochemical behaviour Au NSs/Au and Apt/Au NSs/Au modified electrode

To understand the electrochemical properties of Au NSs/Au and Apt/Au NSs/Au modified electrode, cyclic voltammetry (CV) were carried out with $[Fe(CN)_6]^{3-/4-}$ as a supporting electrolyte. Fig. S3 shows the CV profile of (a) bare Au (b) Au NSs/Au (c) Apt/Au NSs/Au and Apt/MCH/Au NSs/Au in 0.01 M $[Fe(CN)_6]^{3-/4-}$ with 0.1 M KCl as supporting electrolyte in the potential range 0-0.6 V *vs.* Ag/AgCl at a scan rate of 100 mV/s. In the case of bare gold electrode, the peak potential difference (ΔE_p) of 96.2 mV ($I_{pc}/I_{pa} \approx 1$) was observed, which indicates a quasi-reversible redox reaction. Also, the peak current is 4.69 µA. Whereas in the case of Au NSs/Au electrode, the anodic peak current increased considerably (I_p=5.09 µA), which indicates the high redox reaction of $K_3[Fe(CN)_6]$ at the interface due to the thin layer of Au NSs formed at the Au substrate. On the other hand, this is attributed to the reduction of Au(I) to Au(0) at the electrode surface. After the immobilization with aptamer, a small shift in the oxidation peak toward negative potential is obtained with a slight decrement in the redox current, indicating the proper binding of aptamer on Au NSs modified electrode with I_p of 4.22 µA. The decrease in peak current at the electrode interface is attributed to the proper binding of aptamer with Au NSs through the 5′ end SH groups present in the aptamer with the replacement of some of the bulky CTAB adsorbed during cluster formation, which in turn enhance the electron transfer and thus electrochemical activity of the final modified electrode Apt/Au NSs/Au. The changes in the current response during each stage of modification of Au electrode reveals the formation of AuNSs thin film and the proper immobilization of aptamer. Following aptamer incubation, the electrodes were thoroughly rinsed in Tric-HCl (pH 7.4) to remove the unbound aptamer. Then MCH solution (3%) was added to the modified surface and left for 1 h to block the free sites of Apt/AuNSs/Au surfaces to minimize the non-specific binding. Finally, further decrease of the I_p was observed following the MCH blocking of the

Au NSs/Au electrode surface by covering the remaining exposed Au NSs surfaces. The aptasensor were then directly subjected to apta-assay reaction with L-Phe or to electrochemical measurements. Table 1 was summarized all of these parameters for the electrode preparation.

Table 1: Electrochemical parameters for electrode preparation

Index	**Peak position**	**Peak height**
Au	0.23438	4.69
Au/Au NSs	0.23438	5.09
Au/Au NSs/Apt	0.23438	4.22
Au/Au NSs/Apt/MCH	0.23682	3.63

Also, Fig. S4 (A&B) shows CV and DPVs of Au/Au NSs/Apt/MCH in the absence and presence of target molecule (L-Phe), respectively. According to obtained results, in the absence of L-Phe, the peak current is 3.77 by CV technique. But, in the presence of L-Phe the I_p was decrease to 3.44 which confirmed the interaction of Aptamer with target analyte. Therefore, it's obvious that this aptasensor has a suitable ability to detect L-Phe. Similar results were obtained by DPV technique (Fig. S4 B)

3.2.Kinetic study

Scan rate has an important role in the electrochemical behavior of analytes on the electrode surface. On the other hand, scan rate can be used for calculations of special surface coverage (Γ^*), electron transfer coefficient (α) and diffusion or adsorption controlling of mass transfer in the electrochemical systems. Therefore, the effect of scan rate on the electrochemical response of AuNSs/Au electrode was investigated in the presence of $[Fe(CN)_6]^{3-/4-}$. The scan

rate was swept between 20 to 1000 mV/s and the results have been exhibited in Fig. S5A. As it can be seen, the oxidation and reduction peak currents increased proportionally by the scan rate indicating that proposed system has electrocatalytic property. To elucidate the mechanism of mass transfer, two approaches were used. First, the relation between the peak current (mA) and square root of scan rate (V/s) $^{0.5}$ was obtained (Fig. S5B). Using this method, the intercept of the peak current *versus* the square root of scan rate was found to be 0.02, which indicates that the mass transfer is controlled by diffusion mechanism [28] and the system can be applied for quantitative analysis. In the second approach, the Napierian logarithm of peak current (mA) *versus* the Napierian logarithm of scan rate (V/s) was drawn. The results have been illustrated in Fig. S5C. The slops of the plot in Fig. S5C for oxidation peak was found as 0.488. If the slop of ln I_p *versus* ln v (V/s) is close to 0.5, the process is diffusion controlled; if the slope is close to 1, the process is controlled through adsorption [28]. As, the slope was calculated as 0.488, it can be concluded that the mass transfer is a diffusion controlled process which is in agreement with the results of the first approach.

Furthermore, the mass transfer mechanism can also be evaluated by electron transfer coefficient, α, of Eq. 1: [28]

$$Ep = \left(\frac{RT}{2\alpha F}\right) \ln \upsilon + constant \qquad (1)$$

where E_p is electrode potential, R is gas constant (8.314, J $K^{-1}mol^{-1}$), T is temperature in Kelvin scale (298°K), F is Faraday's constant (96486, A.s.mol^{-1}), and υ is potential sweep rate (V/s). If the value of α gets close to 0.5, the system is a diffusion controlled one [28]. Using this equation, the value was obtained as 0.45 which further supports that the mass transfer of the system is controlled by diffusion. In Figs. S5 (E and F), the plot of Eq. 1 obtained from Napierian logarithm of oxidation and reduction peak currents *versus* the corresponding peaks potential (Tafel plot) have been illustrated.

The special surface coverage (Γ^*) was calculated *via* the slop of the oxidation and reduction peak currents (A) *versus* scan rate (V/s) using Eq. 2: [28]

$$Ip = \left(\frac{n^2F^2}{4RT}\right) \upsilon A\Gamma^* \qquad (2)$$

where, n is the number of transferred electron, F is Faraday's constant (96486, A.s.mol^{-1}), R is gas constant (8.314, J K^{-1}mol^{-1}), T is temperature in kelvin scale (298°K), υ is potential sweep rate (V/s), A is total electrode surface(cm^2), and Γ^*(mol cm^{-2}) is special surface covered with AuNSs/Au electrode. Based on the obtained results, the slop of both oxidation and reduction peak currents *versus* sweep rates (Fig. S5G) was 0.00011 and the Γ^* value was calculated as 5.66×10^{-9} mol cm^{-2}. This value is much higher than the corresponding value for bare electrode. When AuNSs was used as the electrode modifier, the Γ^* value was improved. It means that by using AuNSs as electrode modifier, it is possible to increase the efficiency of the proposed biosensor. This improved efficiency could be a result of loading more amounts of aptamer and also an increase in the conductivity of AuNSs/Au.

Also, the stability of the AuNSs/Au electrode in one day and different cycle number (1-100 Cycle) was evaluated by CV techniques. According to obtained results, there is no significant difference on the peak current/potential in different cycle number which confirm the stability of the AuNSs prepared on the surface of gold electrode (Fig. S6).

3.3. Analytical performance

The performance of prepared aptasensor for the detection of L-Phe at different concentrations and its repeatability were evaluated. Fig. S7A depicts the DPVs of the proposed aptasensor obtained for the different concentrations of L-Phe under physiological conditions of pH 7.4 in 0.1 M PBS. The peak current obtained for Apt/Au NSs/Au electrode at 0.344 V, which is attributed to the reduction of Au (I) to Au (0) at the surface of electrode. This peak current due to reduction of clusters can be used as a probe for sensing the target molecules. From the

DPV curves, it can be seen that the peak current of Apt/Au NSs/Au electrode (1.582 µA, the blank signal, *ie.*, without L-Phe in 0.1 M PBS alone) decreases upon increasing the concentration of L-Phe. The decrease in peak current of Apt/Au NSs/Au electrode can be attributed to the nature of the interface formed by the target L-Phe upon the specific binding with the self-assembled aptamer on the AuNSs/Au. The steric hindrance of the L-Phe at the electrode interface prevents the electron transfer to the electrode surface and act as a barrier for the reduction of Au (I) to Au (0) leading to the decrease in peak current.

Also, the reaction mechanism was exhibited in Scheme 2. As can be seen, at first 2-imino-3-phenylpropanoic acid as an intermediate was generated by oxidation of L-Phe via one electron and one proton. Subsequently, elimination of NH_3 and CO_2 occurred and the benzaldehyde and benzoic acid were formed as main products.

According to results and also above mechanisms, it can be considered that desorption step of the intermediated (according to proposed mechanism-produced from first electron transfer step) and formation of product becomes more probable as the rate-determination step. Such behavior for the electrochemical oxidation of L-Phe was confirmed by the proposed mechanism.

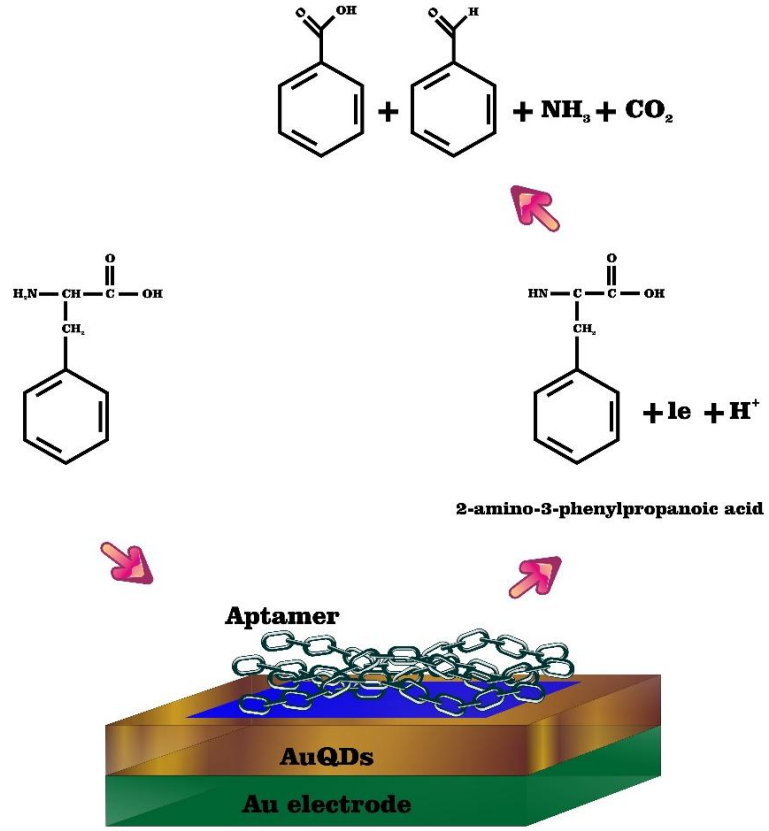

Scheme 2: Oxidation mechanism of L-Phe.

The performance of various electrochemical sensors used for L-Phe detection is summarized in Table 2 [9-11, 20, 22, 29, 30). In comparison with the previous reported methods, the detection limit offered by the current method, is the lowest one. Moreover, the ultra-sensitive Apt/AuNSs/Au electrode can perform with wide calibration range along with high precision, when comparing with any of the previously reported electrochemical L-Phe sensors.

Table 2. Analytical parameters for detection of L-Phe at previously reported methods.

Sensor	Linear Range	LOD[a]	Ref.
Cobalt hydroxide/GCE	30-2000 nM	13.70 nM	9
Fe (III)-Schiff base CN/GCE	9-5000 nM	1.10 nM	22
MCM-41-NH_2/GCE	98-500 nM	13.0 nM	10

Biofunctionalization of Dextran/Enzyme/GCE	0.5-6 mM	0.5 mM	20
Polymer/Enzyme/GCE	0.01-100µM	9 nM	29
MCM-41-Fe_2O_3/GCE	320-510 nM	126 nM	11
Aptamer-Au	1-10 nM	1 nM	30
Apt/AuNSs/Au electrode	0.72 µM-6 mM	0.23 µM	This work

[a] Limit of detection

3.4. Selectivity and stability of the Apt/Au NSs/Au sensor

DPV experiments were carried out to check the cross-reactivity of the L-Phe with possible coexisting and interfering compounds, such as Tyrosine (Tyr), Glycine (Gly), Serine (Ser), L-Valine (L-Ala), Tryptophane (Trp), Arginine (Arg), Proline (Pro), Aspartic acid (Asp), Methionine (Met), and Leucine (Leu). The selectivity of Apt/AuNSs/Au electrode was evaluated in different concentrations of interfering compounds in the supporting electrolyte. For a wide range of concentration of interfering compounds, the ΔI_p% and ΔE_p% produced by the Apt/AuNSs/Au electrode is almost similar (Fig. S8). The successive addition of higher concentrations of interfering compounds did not make any appreciable increment in ΔI_p, unlike in the case of L-Cys and Ascorbic Acid (AA), shows that the proposed sensor exhibits remarkable selectivity towards L-Phe. This can be attributed to the high specificity of the Apt/AuNSs/Au sensor to L-Phe.

The stability of the Apt/AuNSs/Au electrode was also studied by storing the electrode at 4 °C for one week. It was found that 94.11% of the signal was retained, which indicates that the sensor can offer excellent stability (Fig. S9).

3.5. The effect of temperature on electrode stability

Fig. S10 shows the plots for the current response of Apt/Au NSs/Au electrode at various temperatures of the supporting electrolyte. Also, Fig. S10 (B, C) shows dependence of the current/potential response of Apt/Au NSs/Au electrode on the various temperature of supporting electrolyte, respectively. As can be seen, although the current response was changed with increase of the measurement temperature up to 333.15 °K, but the peak potential increases to 303 °K. The applied approach led to better resistance temperature of the aptamer and prepared electrode. The activity of L-Phe specific aptamer immobilized in Au NSs was maintained in the solution temperature up to 303.15 °C.

3.6. Real sample analysis

Real sample analysis were also conducted with human plasma samples. DPV technique was used for the detection procedure (Fig. 6). 1 mL of human plasma samples was diluted in 10 ml of PBS solution and spiked with a known amount of L-Phe. The linearity is obtained from 2.20 nM-5.04 mM due to the matrix effect produced by the L-Phe. The Apt/AuNSs/Au electrode showed excellent recovery for various L-Phe concentrations as 5 mM (99.22%), 2.0 µM (99.14%), 10 µM (97.75%), 5 nM (100.352%) and 2 nM (99.23%) indicating the use of the sensor developed in the real sample analysis.

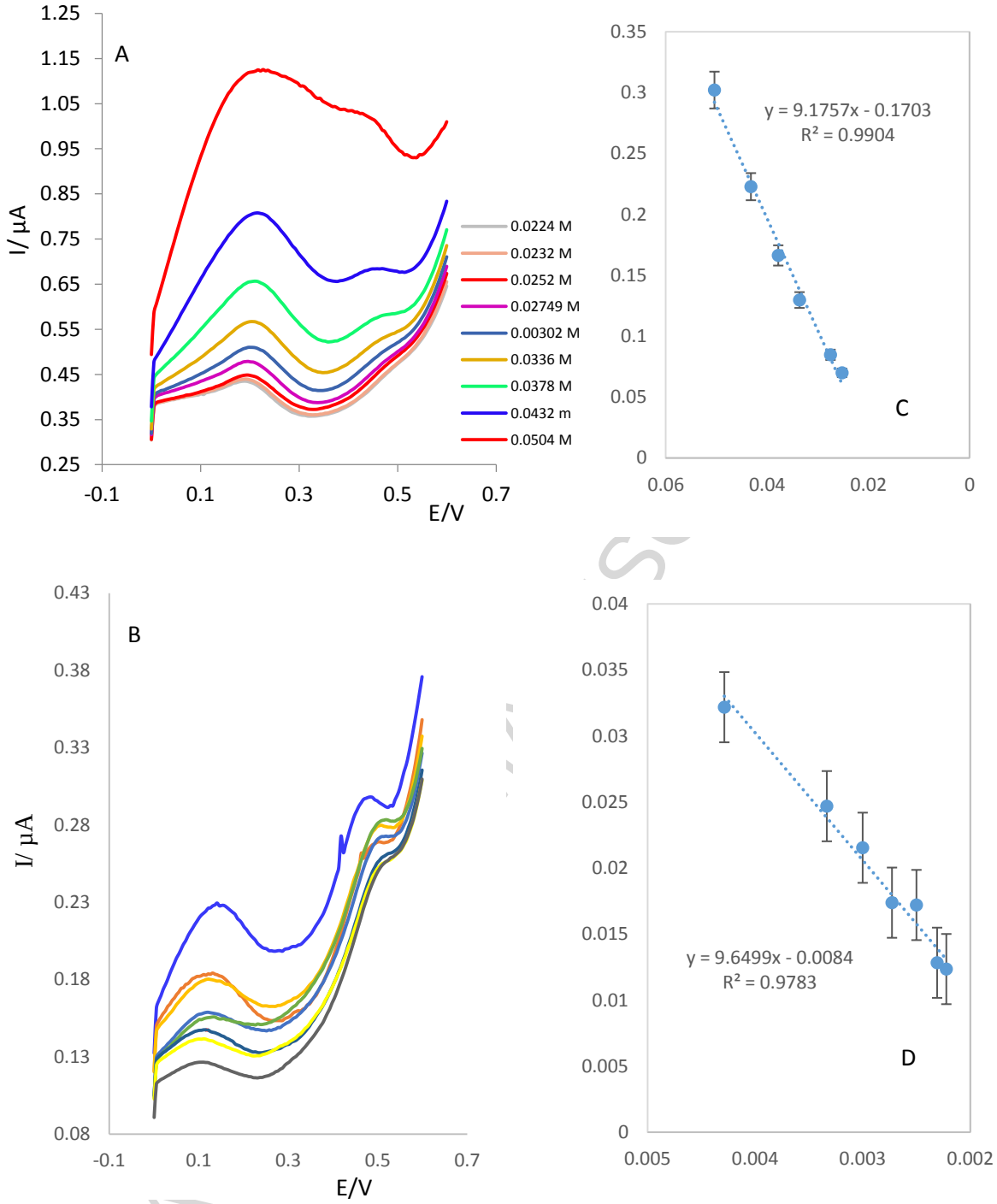

Fig. 6. (**A,B**) DPV plots of the Au/AuNSs/Apt incubated in unprocessed human plasma sample with different concentration of L-Phe in 0.1 M PBS (**A;** 0.02, 0.023, 0.025, 0.027, 0.0302, 0.033, 0.0378, 0.0432, 0.0504 mM, and **B;** 0.0022, 0.0023, 0.0025, 0.00273, 0.003, 0.0033, 0.00429 µM). Supporting electrolyte is 0.1 M PBS (pH=7.4). Pulse amplitude: 0.05 V. Pulse width: 0.05 s. Pulse period: 0.2 s. Scan rate: 5 mVs^{-1}. (**C&D**) Calibration plot *versus* the value of L-Phe concentration.

The concentrations of the three samples in the neonatal plasma samples using the engineered aptasensor (Au/Au NSs/Apt electrode) were measured by DPV technique. The analytical results are shown in Table S1. The data in Table S1 show that the concentrations of L-Phe in the serum samples of phenylketonuria-positive patients were significantly lower than those in control serum samples. Therefore, measurement of L-Phe for phenylketonuria can achieved by analysis of this amino acid in neonatal serum samples using proposed method.

4. Conclusion

In summary, we report for the first time a highly sensitive gold nanostructure mediated electrochemical aptasensor for the detection of L-Phe without any additional signal amplification strategy. The thiolated aptamer was immobilized on the electrochemically synthesized Au NSs on the Au electrode surface, through the strong affinity of 5′end SH groups of the aptamer (Apt) with Au NSs. The SH-gold can form charge-neutral interaction by weak covalent bond, they can also prevent agglomeration of gold nanostructure due to particle stability, which is kinetic rather than thermodynamic in nature. The covalent binding between 5′ end SH groups and Au NSs produces a highly stable electrode Apt/Au NSs/Au for L-Phe detection. We have utilized the allowed or blocked electron transfer through the assembled molecules on the surface to monitor the concentration of target molecule. On taking account of the steric hindrance offered by the L-Phe molecule, a very high sensitivity could be demonstrated. The process of sensor fabrication is very simple when compared with other electrochemical sensors for L-Phe. The developed sensor provided a higher sensitivity than literature reports, and the limit of detection is in pico-molar level.

Acknowledgements

We gratefully acknowledge the financial support by Tabriz University of Medical Sciences.

5. References

[1] N. Al Hafid, J. Christodoulou, Phenylketonuria: a review of current and future treatments, Translational pediatrics 4(4) (2015) 304.

[2] N. Blau, F.J. van Spronsen, H.L. Levy, Phenylketonuria, The Lancet 376(9750) (2010) 1417-1427.

[3] J. Walter, F. White, S. Hall, A. MacDonald, G. Rylance, A. Boneh, D. Francis, G. Shortland, M. Schmidt, A. Vail, How practical are recommendations for dietary control in phenylketonuria?, The Lancet 360(9326) (2002) 55-57.

[4] A.G. DiLella, J. Marvit, A.S. Lidsky, F. Güttler, S.L. Woo, Tight linkage between a splicing mutation and a specific DNA haplotype in phenylketonuria, Nature 322(6082) (1986) 799.

[5] A.J. Bard, L.R. Faulkner, Fundamentals and applications, Electrochemical Methods 2 (2001) 482.

[6] C. Deng, C. Shang, Y. Hu, X. Zhang, Rapid diagnosis of phenylketonuria and other aminoacidemias by quantitative analysis of amino acids in neonatal blood spots by gas chromatography–mass spectrometry, Journal of Chromatography B 775(1) (2002) 115-120.

[7] A.D. Ellington, J.W. Szostak, In vitro selection of RNA molecules that bind specific ligands, nature 346(6287) (1990) 818.

[8] E.E. Ferapontova, E.M. Olsen, K.V. Gothelf, An RNA aptamer-based electrochemical biosensor for detection of theophylline in serum, Journal of the American Chemical Society 130(13) (2008) 4256-4258.

[9] M. Hasanzadeh, G. Karim-Nezhad, N. Shadjou, M. Hajjizadeh, B. Khalilzadeh, L. Saghatforoush, M.H. Abnosi, A. Babaei, S. Ershad, Cobalt hydroxide nanoparticles modified glassy carbon electrode as a biosensor for electrooxidation and determination of some amino acids, Analytical biochemistry 389(2) (2009) 130-137.

[10] M. Hasanzadeh, N. Shadjou, S.-T. Chen, P. Sheikhzadeh, MCM-41-NH2 as an advanced nanocatalyst for electrooxidation and determination of amino acids, Catalysis Communications 19 (2012) 21-27.

[11] M. Hasanzadeh, N. Shadjou, E. Omidinia, Mesoporous silica (MCM-41)-Fe2O3 as a novel magnetic nanosensor for determination of trace amounts of amino acids, Colloids and Surfaces B: Biointerfaces 108 (2013) 52-59.

[12] C. Hendriksz, J. Walter, Update on phenylketonuria, Current Paediatrics 14(5) (2004) 400-406.

[13] T.M. Herne, M.J. Tarlov, Characterization of DNA probes immobilized on gold surfaces, Journal of the American Chemical Society 119(38) (1997) 8916-8920.

[14] Y. Kang, K.-J. Feng, J.-W. Chen, J.-H. Jiang, G.-L. Shen, R.-Q. Yu, Electrochemical detection of thrombin by sandwich approach using antibody and aptamer, Bioelectrochemistry 73(1) (2008) 76-81.

[15] S. Khezrian, A. Salimi, H. Teymourian, R. Hallaj, Label-free electrochemical IgE aptasensor based on covalent attachment of aptamer onto multiwalled carbon nanotubes/ionic liquid/chitosan nanocomposite modified electrode, Biosensors and Bioelectronics 43 (2013) 218-225.

[16] T. Kitagawa, B.A. Smith, E.S. Brown, Gas—Liquid Chromatography of Phenylalanine and Its Metabolites in Serum and Urine of Various Hyperphenylalaninemic Subjects, Their Relatives, and Controls, Clinical chemistry 21(6) (1975) 735-740.

[17] M. Kohlmeier, Nutrient Metabolism: Structures, Functions, and Genes, Academic Press2015.

[18] R. Levicky, T.M. Herne, M.J. Tarlov, S.K. Satija, Using self-assembly to control the structure of DNA monolayers on gold: a neutron reflectivity study, Journal of the American Chemical Society 120(38) (1998) 9787-9792.

[19] L.K. Mahan, S. Escott-Stump, Krause's food & nutrition therapy: Saunders, Elsevier St. Louis, Mo, 2008.

[20] S.M. Naghib, M. Rabiee, E. Omidinia, P. Khoshkenar, Investigation of a Biosensor Based on Phenylalanine Dehydrogenase Immobilized on a Polymer-Blend Film for Phenylketonuria Diagnosis, Electroanalysis 24(2) (2012) 407-417.

[21] S.M. Naghib, M. Rabiee, E. Omidinia, P. Khoshkenara, D. Zeini, Biofunctionalization of dextran-based polymeric film surface through enzyme immobilization for phenylalanine determination, Int. J. Electrochem. Sci 7(1) (2012) 120-135.

[22] L. Saghatforoush, M. Hasanzadeh, N. Shadjou, B. Khalilzadeh, Deposition of new thia-containing Schiff-base iron (III) complexes onto carbon nanotube-modified glassy carbon electrodes as a biosensor for electrooxidation and determination of amino acids, Electrochimica Acta 56(3) (2011) 1051-1061.

[23] M. Hasanzadeh, N. Razmi, A. Mokhtarzadeh, N. Shadjou, S. Mahboob, Aptamer based assay of plated-derived grow factor in unprocessed human plasma sample and MCF-7 breast cancer cell lysates using gold nanoparticle supported α-cyclodextrin, International journal of biological macromolecules 108 (2018) 69-80.

[24] M. Hasanzadeh, N. Shadjou, M. de la Guardia, Aptamer-based assay of biomolecules: recent advances in electro-analytical approach, TrAC Trends in Analytical Chemistry 89 (2017) 119-132.

[25] K. Naoi, Y. Oura, M. Maeda, S. Nakamura, Electrochemistry of surfactant-doped polypyrrole film (I): formation of columnar structure by electropolymerization, Journal of The Electrochemical Society 142(2) (1995) 417-422.

[26] W. Cheng, S. Dong, E. Wang, Synthesis and self-assembly of cetyltrimethylammonium bromide-capped gold nanoparticles, Langmuir 19(22) (2003) 9434-9439.

[27] S. Iijima, T. Ichihashi, Structural instability of ultrafine particles of metals. Phys. Rev. Lett., 56 (6) (1986) 616

[28] L.L. Faulkner, A.J. Bard, Electrochemical Methods and Applications, Wiley2001.

[29] E. Omidinia, N. Shadjou, M. Hasanzadeh, Immobilization of phenylalanine-dehydrogenase on nano-sized polytaurine: A new platform for application of nano-polymeric materials on enzymatic biosensing technology, Materials Science and Engineering: C 42 (2014) 368-373.

[30] E. Omidinia, N. Shadjou, M. Hasanzadeh, Aptamer-based biosensor for detection of phenylalanine at physiological pH, Applied biochemistry and biotechnology 172(4) (2014) 2070-2080.

Highlights

- A novel apta-assay for detection of genetic disorder phenylketonuria (PKU) was successfully developed.
- New platform based on Apt/AuQDs/Au for sensitive detection L-phenylalanine was designed.
- The voltammetric response of the L-phenylalanine exhibited stronger redox, higher current flow, and smaller electron transfer resistance compared with the other type of assays.